

DOI: 10.1002/adma.((please add manuscript number))

Highly Conductive and Stretchable Silver Nanowire Conductors

By *Feng Xu*, and *Yong Zhu**

[*] Prof. Y. Zhu, F. Xu
Department of Mechanical and Aerospace Engineering, North Carolina State University,
Raleigh, North Carolina 27695-7910 (USA)
E-mail: yong_zhu@ncsu.edu

Keywords: Silver nanowire; Stretchable conductor; Buckling; Strain sensor

Materials that are both conductive and stretchable could enable a spectrum of applications such as stretchable displays,^[1] stretchable radiofrequency antennas,^[2] artificial muscles^[3] and conformal skin sensors.^[4-7] A variety of such materials have been recently developed, such as wavy thin metals^[8, 9], metal-coated net-shaped plastic film,^[10] graphene films^[11] and carbon nanotube (CNT)-based composites.^[12-19] But several limitations typically exist in these materials including low conductivity,^[13, 15, 16, 19] poor stretchability,^[10, 11, 16] and resistance increase with applied strain.^[9, 12, 16, 20] As an important alternative strategy, buckled, serpentine structures of metals, encapsulated in neutral mechanical plane layouts by thin polymer coatings, have been fabricated and integrated as interconnects for various stretchable electronic devices.^[21-23] Note that this strategy requires relatively expensive photolithography and metal evaporation in vacuum. More recently, many efforts have been devoted to developing simple, scalable and low-cost methods for fabrication of stretchable conductors.^[24] Wang et al.^[25] reported a novel solution-processing approach to fabricate highly conductive and stretchable conductors. By directly using CNTs^[5] or mixing CNTs with other conductive materials,^[1, 26] other printable and stretchable conductors were also fabricated. However, these stretchable conductive materials are typically deposited on top of substrates and could delaminate under repeated mechanical loading.

As one of the most important conductive materials, Ag nanowires (AgNWs) have recently attracted a lot of attention for potential applications as transparent and flexible electrodes.^[27] Much progress has been made to improve the performance of AgNWs films, including sheet resistance, transparency and flexibility.^[28-35] Hu et al.^[30] achieved optical transmittance $T = 80\%$ and sheet resistance $R_s = 50 \Omega/\square$. Scardaci et al.^[33] demonstrated that AgNWs can be spray deposited over large areas to form networks with $T = 90\%$ and $R_s = 50 \Omega/\square$. Yu et al.^[35] reported large flexibility of AgNW film on polyacrylate substrate under bending; the resistance was nearly unchanged under compressive strain while increased by 2.9

times at a tensile strain of 16%. Yet highly conductive, stretchable and stable conductors based on AgNWs have not been achieved.^[36]

In this paper, we report a highly conductive and stretchable conductor with AgNWs embedded in the surface layer of poly(dimethylsiloxane) (PDMS). The conductivity is $\sim 8,130$ S cm⁻¹ (sheet resistance of 0.24 Ω/\square) before stretched. After a few stretching/releasing cycles, the resistance of our AgNW/PDMS conductor becomes stable in the tensile strain range of 0-50%, still with a very high conductivity of 5,285 S cm⁻¹. The physics/mechanics origin of such stable conductance is investigated. The stretchable conductors show excellent robustness under repeated mechanical loading. Moreover, the AgNWs are in solution, which makes them easily compatible with existing parallel or serial fabrication/patterning techniques. A stretchable LED circuit and a capacitive strain sensor are demonstrated using the AgNW-based stretchable conductors.

The fabrication process of the AgNW/PDMS stretchable conductor is schematically illustrated in **Figure 1a**. Initially, AgNWs suspension in ethanol is drop-casted onto a precleaned substrate. The substrate could be silicon (Si) wafer, glass slide or plastic materials. The AgNWs are then dried to form a uniform and conductive film of AgNW network with thickness ranging from one to several micrometers. Next, liquid PDMS is casted on top of the AgNW film, followed by curing at 65 °C for 12 h. When peeled off the substrate, the AgNW film is bonded to the cured PDMS. The AgNW film is actually buried just below the PDMS surface (i.e., the top surface is a composite of AgNWs and PDMS), forming a conductive and stretchable layer.

Figure 1b shows the top-view SEM image of AgNWs coating on the original substrate (Si wafer in this case), where a dense network of randomly oriented AgNWs is seen. The AgNWs have average diameter of ~ 90 nm and length in the range of 10-60 μm . Figure 1c shows the top-view SEM image of AgNWs after being transferred and embedded to PDMS substrate. Only scarce AgNWs on the very top of the PDMS surface is observable; the

majority of the AgNWs are buried below the surface. When the liquid PDMS is poured onto the AgNW film, the liquid penetrates into the AgNW network, owing to its low viscosity and low surface energy. When the PDMS cures, it becomes highly cross-linked with the AgNWs embedded. The sheet resistance of AgNW films before and after casting the PDMS was also examined, and an average of 30% increase was found. The pouring of PDMS onto the AgNW film might lead to filling of PDMS at the NW junctions, thus increasing the effective resistance of the NW network. However, the AgNW/PDMS layer still has a very high conductivity of $8,130 \text{ S cm}^{-1}$ before stretching. Thanks to the PDMS matrix, the intrinsically fragile AgNW network was mechanically robust. No delamination, wear or increase in resistance was observed after repeated stretching, adhesion against tapes and rubbing on the surface.

To test its performance as a stretchable conductor, the PDMS substrate along with the AgNW/PDMS layer was stretched by a tensile testing stage,^[17, 37] while the electric resistance was measured at the same time. Figure S1 shows the AgNW/PDMS film under tensile strain of 0%, 50% and 80%. Eutectic gallium-indium (EGaIn, Aldrich, $\geq 99.99\%$) was applied to the two ends of the AgNW/PDMS film to serve as conformal electrodes (Figure S1).^[5] Figure 1d shows the resistance as a function of the applied strain. It can be seen that the resistance first increased almost linearly from 0.82 to 3.77Ω when the tensile strain increased to 80%. Upon release of the strain, the resistance was partially recovered and decreased to 2.67Ω when the PDMS was fully released. Subsequently when the PDMS was stretched back to 80% strain, the resistance remained nearly constant up to 50%. However, beyond 50% strain, the resistance increased linearly again with the strain, following the same path as in the first stretching. More stretching/releasing cycles in the strain range of 0-50% were performed. The resistance showed no change in each stretching cycle, while decreased slightly in each releasing cycles. A stable resistance was achieved by the fifth stretching/releasing cycle and remained unchanged for more cycles within the strain range of 0-50%. Figure 1e shows the

resistances in the fifth and fortieth stretching cycles. The conductivity was found to remain as high as 5285 S cm^{-1} at strain of 50%. This stretchability is superior to the gold thin film on PDMS deposited by e-beam evaporation.^[20] The stretchable range with stable resistance is comparable to that of the CNT-based stretchable conductors while the conductivity is much higher especially at the stretched state.^[1, 13, 15, 19, 26] Notably, similar resistance change behavior was observed when the same AgNW/PDMS film was subjected to stretching along the other axis; stable resistance was achieved in the strain range up to 30%.

To probe the mechanism of the observed resistance behavior under mechanical strain, the surface morphology of the AgNW/PDMS layer was monitored *in situ* during a stretching/releasing/re-stretching cycle via optical microscopy. Optical images corresponding to different applied strains during the stretching/releasing cycle are provided in the supporting information. **Figure S2a** shows the AgNW/PDMS layer before stretching. It can be seen that the surface of the AgNW/PDMS layer is flat without any noticeable undulation. When the PDMS was stretched, the surface morphology did not show obvious change; see Figure S2b as an example for 80% strain. When the strain was released, surface buckling (wrinkling) started to appear in the stretching direction at $\sim 50\%$ strain (Figure S2c). More buckles appeared with further release of the strain; the buckle amplitude and wavelength increased and decreased, respectively (Figure S2d). When the PDMS was stretched again, the amplitude and wavelength of the surface buckles gradually decreased and increased, respectively. At $\sim 50\%$ strain, the surface buckles almost disappeared. The surface morphology remained unchanged up to 80% strain. Note that no cracking was observed until the fracture the PDMS up to strain of more than 100%. Surface morphology of the AgNW/PDMS layer after stretching/releasing cycles was further examined by SEM (**Figure 2a** and b). Similar to the observation from optical images, a periodic wavy pattern appeared on the surface of the AgNW/PDMS layer, in contrast to the flat surface before stretching. The cross-sectional SEM image in Figure 2b reveals that the wavy structure is due to buckling of the top AgNW/PDMS

layer on the PDMS substrate. No debonding or cracks between the AgNW/PDMS layer and the PDMS body was observed. The buckled wavy shape of the AgNW/PDMS layer is responsible for the observed stable resistance in the large strain range of 0-50%. The morphology change of the AgNW/PDMS layer after being stretched and released along the other axis is shown in Figure S3.

Electric resistance of an AgNW network can be substantially influenced by the contacts between NWs.^[30] When the AgNW/PDMS layer is first stretched, AgNWs might slide between each other, as schematically illustrated in Figure 2c-d. The weakening and detachment of the NW contacts results in a smaller overall contact area between NWs, thus leading to the increase of resistance. It has been reported that the fracture strains of the AgNWs with different diameters are in the range of 0.92%-1.64%,^[38] which is very small compared with the strains we applied on the stretchable conductor. Therefore, the contribution of the NW plastic deformation to the observed resistance change under strain is negligible. When the AgNW/PDMS layer is released, the AgNWs slide back by certain degree but cannot slide back to the initial state because of the friction force between the NWs and the PDMS matrix; rather the AgNW/PDMS layer buckles out of plane as a whole (Figure 2f). Indeed a residual strain exists in the AgNW/PDMS layer upon unloading, which was found to be around 50% (Figures 2e and S1c). An irreversible fiber arrangement and residual strain has also been observed in networks of CNTs^[39] and other fibers.^[40] This scenario is now resembling to the prestraining approach used in stretchable electronics:^[21, 37] the AgNW/PDMS layer is positioned on top of a PDMS substrate that is prestrained by 50%. Upon further release of the strain, the AgNW/PDMS layer buckles into a wavy, sinusoidal shape. As a result of the buckling, the resistance of the AgNW/PDMS layer does not change during releasing from 50% to zero strain. The second stretching is essentially flattening of the buckled AgNW/PDMS layer (up to 50% strain), which accompanies a constant resistance as expected. Beyond 50% strain, the sliding between NWs occurs again so that the resistance

increases linearly following the same path as in the first stretching. This electric response is somewhat similar to that of aligned CNT ribbons,^[14, 17] but the sliding mechanism and the buckling mode are very different. We have also tried another commonly used strategy to fabricate stretchable conductors by prestraining the PDMS substrate and then drop-casting the AgNW films. However, due to the weak adhesion between the AgNW film and the PDMS surface, delamination occurred during the strain release.

The AgNW film can be printed to fabricate patterned stretchable conductors. As a demonstration, we began with depositing AgNW lines on Si substrate through a shadow mask. After removing the shadow mask, the patterned AgNW lines were embedded in PDMS and then peeled off following the same procedure as illustrated in Figure 1a. **Figure 3a** shows the parallel AgNW/PDMS elastic conductors with a linewidth of 800 μm ; the performance was found to be the same as that of the conductor in Figure 1d and e, in terms of both stretchability and conductivity. The inset of Figure 3a shows the conductors deformed by hand. Crossed patterns were also fabricated (Figure 3b). Several more examples showing different patterns and linewidth as small as 50 μm can be found in the Figure S4. With two patterned AgNW/PDMS lines, we constructed a simple circuit to power a light-emitting diode (LED), as shown in Figure 3c. The LED remained lit with the same illumination intensity as the AgNW/PDMS conductors were stretched to a strain of 50% (Figure 3d) or folded (Figure 3e).

Furthermore, with the above patterning technology, a strain sensor was fabricated with the configuration similar to a parallel-plate capacitor (**Figure 4a**). The device comprised a PDMS slab with two patterned AgNW strips embedded in the top and bottom surfaces, as two stretchable electrodes. The thickness of each AgNW/PDMS strip was 3 μm while the spacing between them was about 1 mm. The initial capacitance of the sensor was given by

$$C_0 = \varepsilon_0 \varepsilon_r \frac{A_0}{d_0},$$

where ε_0 is the electric constant, ε_r is the dielectric constant, and A_0 and d_0

are the area overlap and separation between the two electrodes, respectively. When the sensor was uniaxially stretched, the change in capacitance ΔC due to an applied strain ε is given by $\Delta C = C_0 \varepsilon$ (see supporting information). Figure 4b plots the capacitance change as a function of the applied strain (up to 50%). The capacitance increase is about the same as the strain, which is in good agreement with the theoretical prediction.

Our strain sensor shows excellent linearity under a very large strain range. The gauge factor of our strain sensor ($\Delta C/C/\varepsilon$) is about 1 and the minimum detectable strain is <1% (Figure 4b). For the sake of comparison, the gauge factors reported by Yamada et al.^[41] for stretchable films of aligned CNTs (in resistor configuration) were 0.82 (0 to ~40% strain) and 0.06 (~60 to 200%). A gauge factor of ~0.4 was reported by Lipomi et al.^[5] for sprayed CNT films (in parallel-plate configuration), though the sensor was not sensitive enough to detect strains less than 10%. Figure 4c shows capacitance versus time for four cycles of applied strain up to 20%, showing stable response of our strain sensor. The large strain range is unmatched by conventional strain gauges.

In summary, AgNW-based stretchable conductors were fabricated by embedding AgNWs just below the surface of PDMS. A stable conductivity of 5,285 S cm⁻¹ was achieved after a few cycles of stretching/releasing in a large range of tensile strain (0-50%). This stable electrical response is due to buckling of the AgNW/PDMS layer. The physics/mechanics origin of the buckling is due to irreversible sliding of the AgNWs in the PDMS matrix. Following a parallel fabrication approach, line and cross patterns of AgNWs were fabricated. Furthermore, a stretchable LED circuit and a capacitive strain sensor were demonstrated using the AgNW/PDMS elastic conductors as interconnects or electrodes. With their superior conductivity, stretchability and compatibility with existing fabrication/patterning technology, the reported AgNW/PDMS elastic conductors may find broad applications in stretchable electronics, skin sensors, wearable communication devices, photovoltaics and energy storage. Transparent electrodes using AgNWs have also received much attention recently. It remains a

significant challenge to achieve high conductivity, transparency and stretchability simultaneously.

Experimental Section

Sample preparation:

AgNWs were provided by Blue Nano, Inc. PDMS were prepared using Sylgard 184 (Dow Corning) by mixing the “base” and the “curing agent” with a ratio of 10:1. After air bubbles disappeared, the liquid mixture was then thermally cured at 65 °C for 12 hours to form cross-linked and solid PDMS.

Fabrication and measurement of capacitive strain sensors:

Liquid PDMS layer was first casted onto a Si substrate patterned with rectangular AgNW films. Before curing, we placed an already patterned and cured AgNW/PDMS film (with the AgNW surface facing up) on the Si substrate as well as the wet PDMS and oriented it to make sure that both patterns are perfectly aligned. Following that, the whole piece was thermally cured and peeled off the Si substrate. This way, the top and bottom surfaces of the PDMS were symmetrically covered by the patterned AgNW stretchable electrodes. Cutting a strip off the PDMS substrate produced a capacitive strain sensor, as schematically shown in Figure 4a. The strain sensor were repeatedly stretched and released by a tensile testing stage (Ernest F. Fullam), while the capacitance was measured at the same time by a LCR (inductance, capacitance, resistance) meter (Stanford Research Systems, SR715).

Acknowledgements

This work was partially supported by the National Science Foundation under Award No. CMMI-1030637. The authors are grateful to Blue Nano Inc. and Prof. Michael Dickey for providing the AgNWs.

References

- [1] T. Sekitani, H. Nakajima, H. Maeda, T. Fukushima, T. Aida, K. Hata, T. Someya, *Nat. Mater.* **2009**, *8*, 494.
- [2] M. Kubo, X. F. Li, C. Kim, M. Hashimoto, B. J. Wiley, D. Ham, G. M. Whitesides, *Adv. Mater.* **2010**, *22*, 2749.
- [3] A. E. Aliev, J. Oh, M. E. Kozlov, A. A. Kuznetsov, S. Fang, A. F. Fonseca, R. Ovalle, M. D. Lima, M. H. Haque, Y. N. Gartstein, M. Zhang, A. A. Zakhidov, R. H. Baughman, *Science* **2009**, *323*, 1575.
- [4] D. H. Kim, N. S. Lu, R. Ma, Y. S. Kim, R. H. Kim, S. D. Wang, J. Wu, S. M. Won, H. Tao, A. Islam, K. J. Yu, T. I. Kim, R. Chowdhury, M. Ying, L. Z. Xu, M. Li, H. J. Chung, H. Keum, M. McCormick, P. Liu, Y. W. Zhang, F. G. Omenetto, Y. G. Huang, T. Coleman, J. A. Rogers, *Science* **2011**, *333*, 838.
- [5] D. J. Lipomi, M. Vosgueritchian, B. C. Tee, S. L. Hellstrom, J. A. Lee, C. H. Fox, Z. Bao, *Nat. Nanotechnol.* **2011**, *6*, 788.
- [6] S. Wagner, S. P. Lacour, J. Jones, P. H. I. Hsu, J. C. Sturm, T. Li, Z. G. Suo, *Physica E-Low-Dimensional Systems & Nanostructures* **2004**, *25*, 326.
- [7] K. Takei, T. Takahashi, J. C. Ho, H. Ko, A. G. Gillies, P. W. Leu, R. S. Fearing, A. Javey, *Nat. Mater.* **2010**, *9*, 821.
- [8] N. Bowden, S. Brittain, A. G. Evans, J. W. Hutchinson, G. M. Whitesides, *Nature* **1998**, *393*, 146.
- [9] D. S. Gray, J. Tien, C. S. Chen, *Adv. Mater.* **2004**, *16*, 393.
- [10] T. Someya, Y. Kato, T. Sekitani, S. Iba, Y. Noguchi, Y. Murase, H. Kawaguchi, T. Sakurai, *Proc. Natl. Acad. Sci. U.S.A.* **2005**, *102*, 12321.
- [11] K. S. Kim, Y. Zhao, H. Jang, S. Y. Lee, J. M. Kim, K. S. Kim, J. H. Ahn, P. Kim, J. Y. Choi, B. H. Hong, *Nature* **2009**, *457*, 706.
- [12] L. B. Hu, W. Yuan, P. Brochu, G. Gruner, Q. B. Pei, *Appl. Phys. Lett.* **2009**, *94*, 161108.
- [13] M. K. Shin, J. Oh, M. Lima, M. E. Kozlov, S. J. Kim, R. H. Baughman, *Adv. Mater.* **2010**, *22*, 2663.
- [14] Y. Y. Zhang, C. J. Sheehan, J. Y. Zhai, G. F. Zou, H. M. Luo, J. Xiong, Y. T. Zhu, Q. X. Jia, *Adv. Mater.* **2010**, *22*, 3027.
- [15] K. H. Kim, M. Vural, M. F. Islam, *Adv. Mater.* **2011**, *23*, 2865.
- [16] K. Liu, Y. H. Sun, P. Liu, X. Y. Lin, S. S. Fan, K. L. Jiang, *Adv. Funct. Mater.* **2011**, *21*, 2721.
- [17] Y. Zhu, F. Xu, *Adv. Mater.* **2012**, *24*, 1073.
- [18] F. Xu, X. Wang, Y. T. Zhu, Y. Zhu, *Adv. Funct. Mater.* **2012**, *22*, 1279.
- [19] T. Sekitani, Y. Noguchi, K. Hata, T. Fukushima, T. Aida, T. Someya, *Science* **2008**, *321*, 1468.
- [20] S. P. Lacour, S. Wagner, Z. Y. Huang, Z. Suo, *Appl. Phys. Lett.* **2003**, *82*, 2404.
- [21] D. H. Kim, J. Xiao, J. Song, Y. Huang, J. A. Rogers, *Adv. Mater.* **2010**, *22*, 2108.
- [22] J. A. Rogers, T. Someya, Y. G. Huang, *Science* **2010**, *327*, 1603.
- [23] D. H. Kim, J. Z. Song, W. M. Choi, H. S. Kim, R. H. Kim, Z. J. Liu, Y. Y. Huang, K. C. Hwang, Y. W. Zhang, J. A. Rogers, *Proc. Natl. Acad. Sci. U.S.A.* **2008**, *105*, 18675.
- [24] B. Y. Ahn, E. B. Duoss, M. J. Motala, X. Y. Guo, S. I. Park, Y. J. Xiong, J. Yoon, R. G. Nuzzo, J. A. Rogers, J. A. Lewis, *Science* **2009**, *323*, 1590.

- [25] X. L. Wang, H. Hu, Y. D. Shen, X. C. Zhou, Z. J. Zheng, *Adv. Mater.* **2011**, *23*, 3090.
- [26] K. Y. Chun, Y. Oh, J. Rho, J. H. Ahn, Y. J. Kim, H. R. Choi, S. Baik, *Nat. Nanotechnol.* **2010**, *5*, 853.
- [27] D. S. Hecht, L. Hu, G. Irvin, *Adv. Mater.* **2011**, *23*, 1482.
- [28] J. Y. Lee, S. T. Connor, Y. Cui, P. Peumans, *Nano Lett.* **2008**, *8*, 689.
- [29] S. De, T. M. Higgins, P. E. Lyons, E. M. Doherty, P. N. Nirmalraj, W. J. Blau, J. J. Boland, J. N. Coleman, *ACS Nano* **2009**, *3*, 1767.
- [30] L. B. Hu, H. S. Kim, J. Y. Lee, P. Peumans, Y. Cui, *Acs Nano* **2010**, *4*, 2955.
- [31] X. Y. Zeng, Q. K. Zhang, R. M. Yu, C. Z. Lu, *Adv. Mater.* **2010**, *22*, 4484.
- [32] W. Gaynor, G. F. Burkhard, M. D. McGehee, P. Peumans, *Adv. Mater.* **2011**, *23*, 2905.
- [33] V. Scardaci, R. Coull, P. E. Lyons, D. Rickard, J. N. Coleman, *Small* **2011**, *7*, 2621.
- [34] Z. Yu, L. Li, Q. Zhang, W. Hu, Q. Pei, *Adv. Mater.* **2011**, *23*, 4453.
- [35] Z. B. Yu, Q. W. Zhang, L. Li, Q. Chen, X. F. Niu, J. Liu, Q. B. Pei, *Adv. Mater.* **2011**, *23*, 664.
- [36] S. Yun, X. Niu, Z. Yu, W. Hu, P. Brochu, Q. B. Pei, *Adv. Mater.* **2012**, DOI: 10.1002/adma.201104101.
- [37] F. Xu, W. Lu, Y. Zhu, *ACS Nano* **2011**, *5*, 672.
- [38] Y. Zhu, Q. Q. Qin, F. Xu, F. R. Fan, Y. Ding, T. Zhang, B. J. Wiley, Z. L. Wang, *Phys. Rev. B* **2012**, *85*.
- [39] P. Slobodian, P. Riha, A. Lengalova, P. Saha, *J. Mater. Sci.* **2011**, *46*, 3186.
- [40] D. Poquillon, B. Viguier, E. Andrieu, *J. Mater. Sci.* **2005**, *40*, 5963.
- [41] T. Yamada, Y. Hayamizu, Y. Yamamoto, Y. Yomogida, A. Izadi-Najafabadi, D. N. Futaba, K. Hata, *Nat. Nanotechnol.* **2011**, *6*, 296.

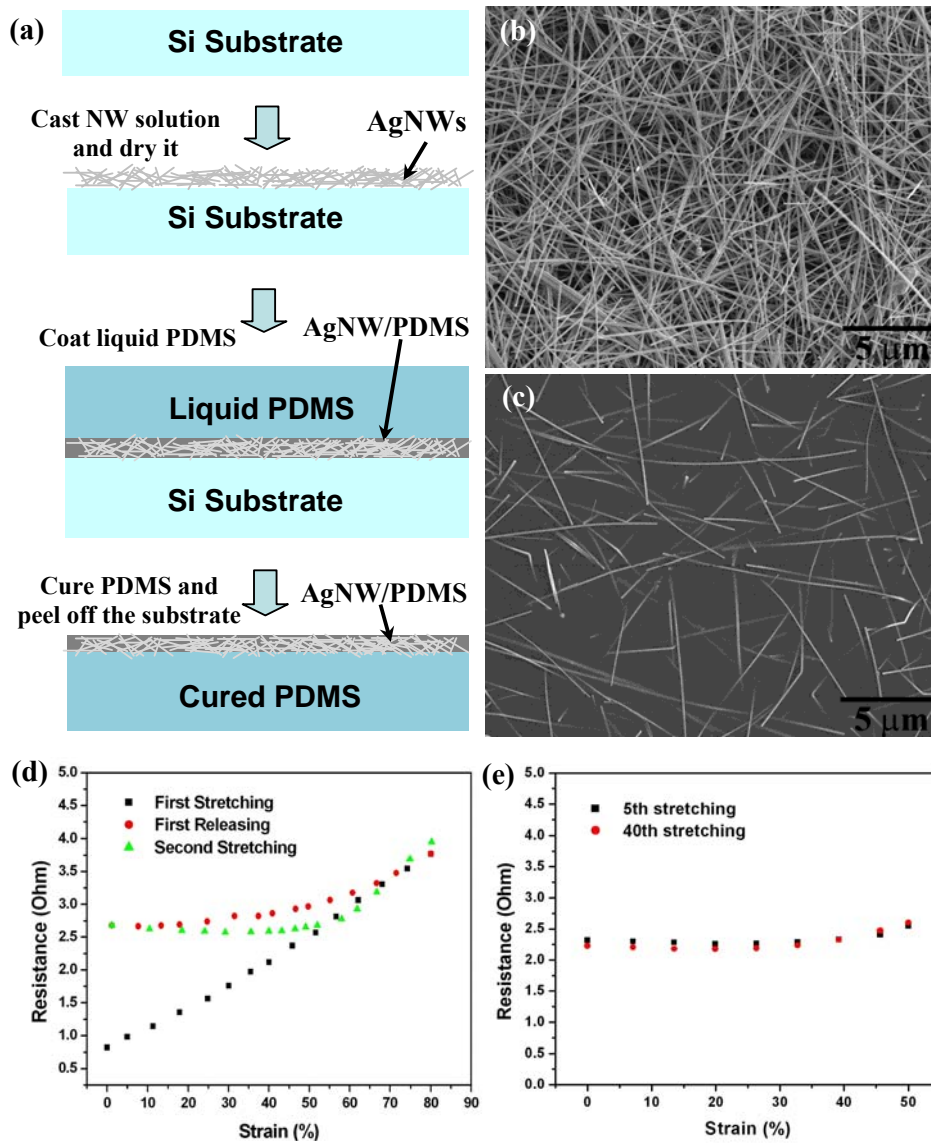


Figure 1. (a) A schematic showing the fabrication process of the AgNW/PDMS stretchable conductors. (b) SEM image of the AgNW film on Si substrate. (c) SEM image of the AgNW film after transferred to PDMS substrate. (d) Resistance of an AgNW/PDMS stretchable conductor as a function of tensile strain. (e) Resistances as a function of tensile strains (0-50%) for the AgNW/PDMS stretchable conductor in the fifth and fortieth stretching cycles.

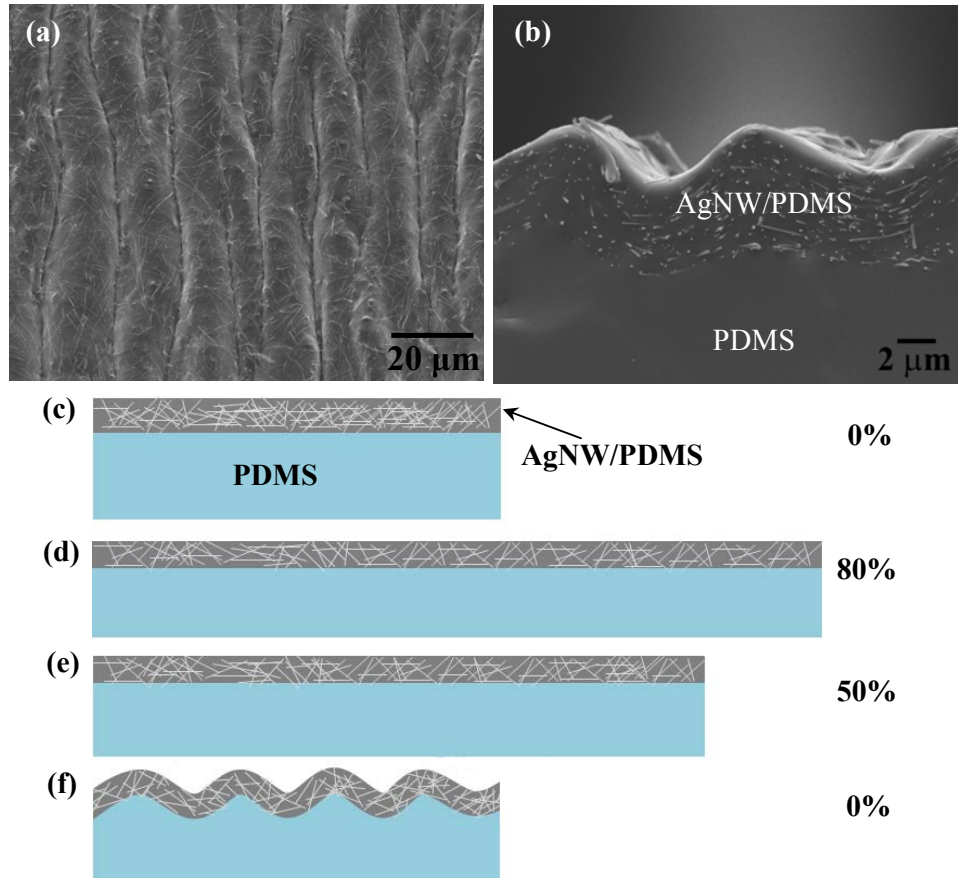


Figure 2. (a) SEM image of the AgNW/PDMS surface after the stretching and releasing cycles. The image was taken by tilting the sample at an angle of 20° . (b) Cross-sectional SEM image of the AgNW/PDMS layer. A Schematic showing the deformation of AgNW/PDMS layer during the stretching (c-d) and releasing (d-f) process, in corresponding to the optical observation in Figure S2. The corresponding strain is also indicated on the right.

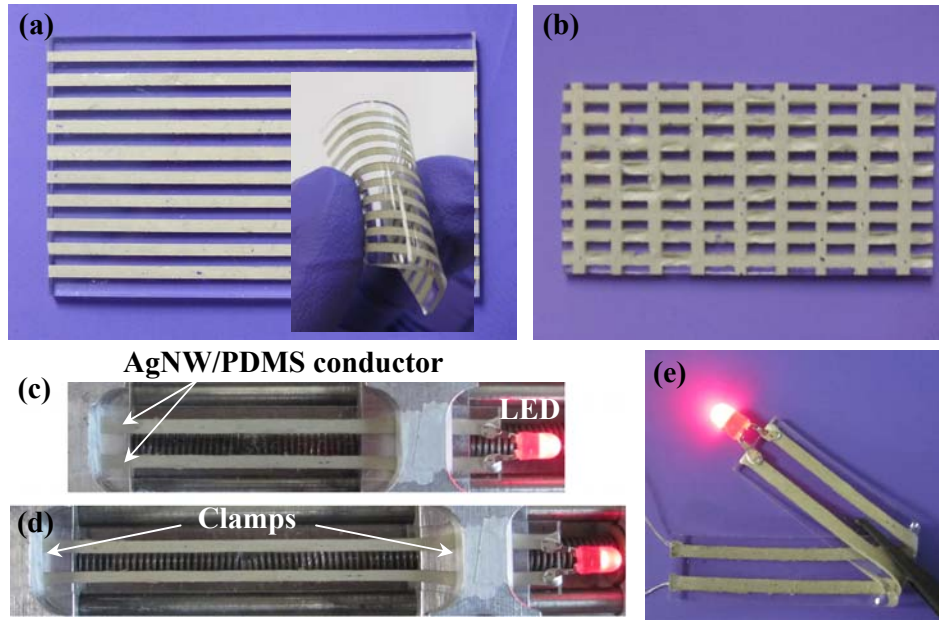


Figure 3. (a) Patterned parallel AgNW/PDMS stretchable conductors with linewidth of 800 μm . The inset shows the conductors deformed by hand. (b) Crossed patterns of AgNW/PDMS stretchable conductors. (c, d) Optical photograph of the LED integrated circuit under tensile strain of 0% and 50%. The two AgNW/PDMS elastic conductors are clamped on a mechanical testing stage. The other ends of the AgNW/PDMS lines were connected to a 1.7 V battery. (e) Optical photograph of the LED integrated circuit under folding.

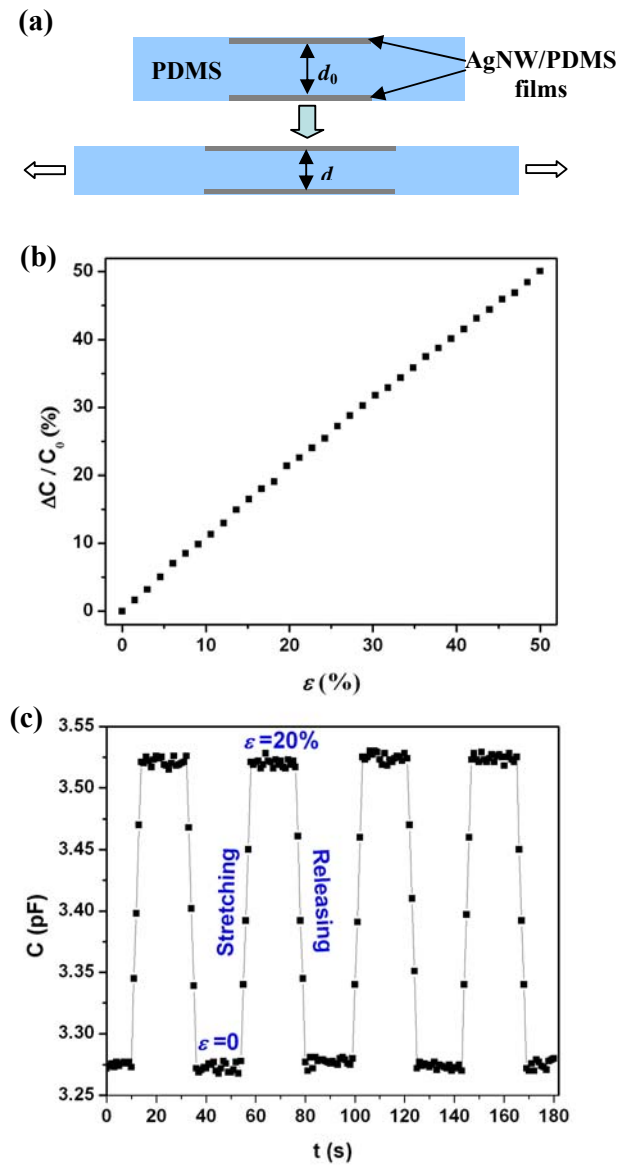


Figure 4. (a) Schematic showing a capacitive strain sensor with AgNW/PDMS layer as the electrodes (top) before and (bottom) after being stretched. (b) Change in capacitance $\Delta C/C_0$ versus tensile strain ϵ . (c) Capacitance C versus time t over four cycles of stretching and releasing.

Supporting Information**AgNW/PDMS film under tensile strain**

Figure S1 shows the AgNW/PDMS film under tensile strain of 0%, 50% and 80%. Eutectic gallium-indium (EGaIn, Aldrich, $\geq 99.99\%$) was applied to the two ends of the AgNW/PDMS film to serve as conformal electrodes.

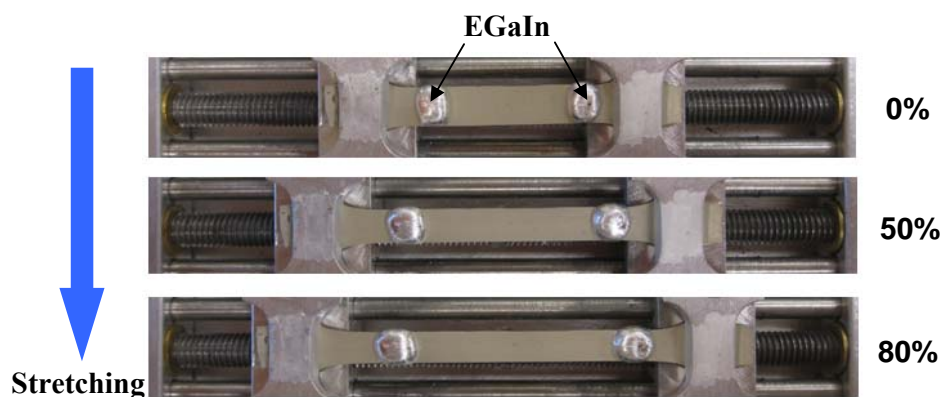


Figure S1. Optical photographs of an AgNW/PDMS stretchable conductor under tensile strains of 0%, 50% and 80%.

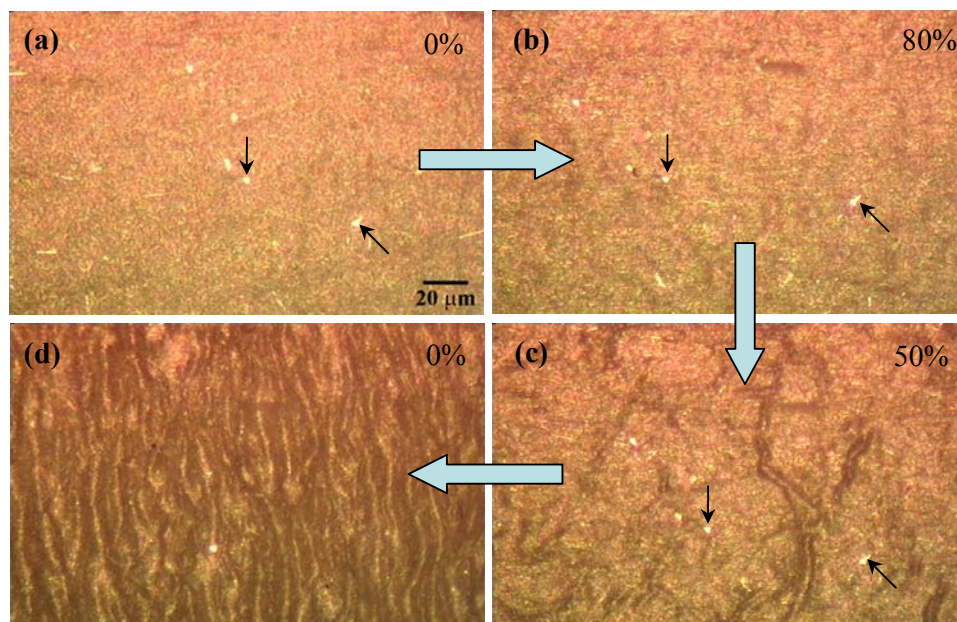
Surface morphology evolution of the AgNW/PDMS layer

Figure S2. Top view optical images showing the surface morphology of the AgNW/PDMS layer during the stretching (a-b) and releasing (b-d) process. In the top right corner of each image is the corresponding strain. Two dots in each panel are arrowed as reference marks. All the images are taken at the same magnification (scale bar is shown in panel a).

Biaxial stretching

The morphology change of the buckled AgNW/PDMS layer after being stretched and released along the other in-plane axis was also investigated. As shown in Figure S3, buckles were also found to form along the other axis.

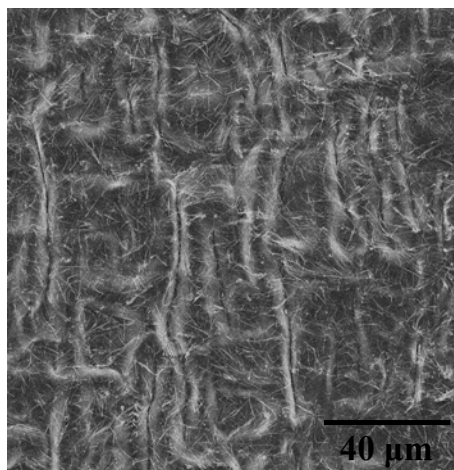


Figure S3. Top view SEM image showing the surface morphology of the AgNW/PDMS layer after being stretched and released along the other axis.

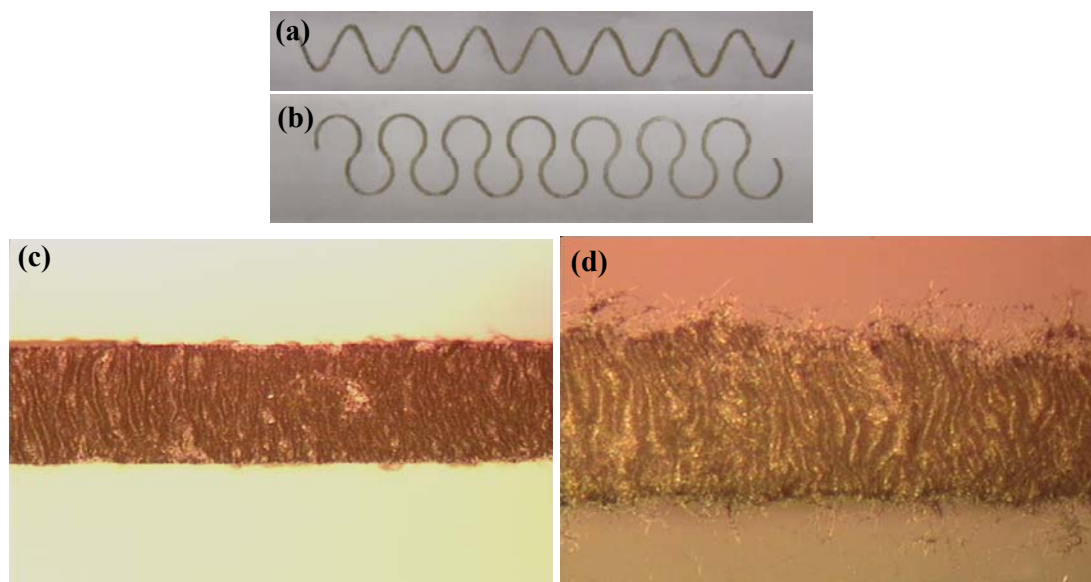
A couple of more examples showing different patterns and linewidth

Figure S4. Optical photographs of patterned (a) wavy and (b) horseshoe shaped AgNW/PDMS stretchable conductors with the same wavelength of 2.5 mm and linewidth of 200 μm . (c, d) Optical images showing the AgNW/PDMS stretchable conductor lines with linewidth of 100 and 50 μm , respectively. The patterns were fabricated with the assistance of PDMS made shadow masks as cut by a laser cutter.

Analysis of the capacitance change with strain

The initial capacitance of the sensor is given by $C_0 = \varepsilon_0 \varepsilon_r \frac{A_0}{d_0} = \varepsilon_0 \varepsilon_r \frac{l_0 w_0}{d_0}$, where ε_0 is the electric constant, ε_r the dielectric constant, A_0 the area overlap, l_0 and w_0 the length and width of the area overlap, respectively, and d_0 the separation between the two electrodes. According to linear elasticity theory, when the sensor is uniaxially stretched to a strain of ε , l_0 increases to $(1+\varepsilon)l_0$ while w_0 and d_0 respectively decrease to $(1-\nu\varepsilon)w_0$ and $(1-\nu\varepsilon)d_0$, where ν is Poisson ratio of the PDMS. Thus, the capacitance with the applied strain changes to

$$C = \varepsilon_0 \varepsilon_r \frac{(1+\varepsilon)l_0(1-\nu\varepsilon)w_0}{(1-\nu\varepsilon)d_0} = \varepsilon_0 \varepsilon_r \frac{(1+\varepsilon)l_0 w_0}{d_0} = (1+\varepsilon)C_0.$$

Therefore, the change in capacitance ΔC due to an applied strain ε is given by $\Delta C = C_0 \varepsilon$. The same results can be obtained following nonlinear elasticity theory.